Journal of Pharmaceutical Sciences 106 (2017) 3033-3040

Contents lists available at ScienceDirect

Journal of Pharmaceutical Sciences

journal homepage: www.jpharmsci.org

Pharmaceutics, Drug Delivery and Pharmaceutical Technology

Application of 1-Dimensional and 2-Dimensional Solid-State Nuclear Magnetic Resonance Spectroscopy to the Characterization of Morphine, Morphine Hydrochloride, and Their Hydrates

Carolina B. Romañuk [1], Yamila Garro-Linck [2], M. Silmara Alves de Santana [3], Ruben H. Manzo [1], Alejandro P. Ayala [3], Gustavo A. Monti [2], Ana K. Chattah [2], Maria E. Olivera [1, *]

[1] Unidad de Investigación y Desarrollo en Tecnología Farmacéutica (UNITEFA), CONICET y Departamento de Farmacia, Facultad de Ciencias Químicas-UNC, Córdoba, Argentina
[2] Instituto de Física Enrique Gaviola (IFEG), CONICET y Facultad de Matemática, Astronomía y Física-UNC, Córdoba, Argentina
[3] Centro de Ciências, Departamento de Física, Universidade Federal do Ceará, Fortaleza, Brazil

ARTICLE INFO

Article history:
Received 15 February 2017
Revised 24 April 2017
Accepted 8 May 2017
Available online 24 May 2017

Keywords:
solid-state characterization
opioids
hydrogen bond
spectroscopy
salts

ABSTRACT

The detailed knowledge of the solid forms of a drug is a key element in pharmaceutical development. Morphine (MOR) is an opiate alkaloid widely used to treat severe acute and chronic pain. Much of the available information on its solid state dates from several decades ago. In order to obtain updated and reliable information, 1-dimensional (1D) and 2-dimensional solid-state nuclear magnetic resonance spectroscopy were used and complemented with powder X-ray diffraction, FTIR, and Raman spectroscopy and thermal analysis. ^{13}C cross-polarization with magic angle spinning 1D spectra accomplish a complete identification of the related forms of MOR. Remarkably, ^{1}H-^{13}C heteronuclear correlation spectra together with FTIR results gave clear evidence that neither MOR nor its hydrate crystallizes as a zwitterion. Our results indicate that the hydrogen bonds in the anhydrate forms have a different nature or strength than in their respective hydrates. The unique information obtained would be useful for the characterization of MOR as a bulk drug, dosage forms, and future developments.

Introduction

The solid-state chemistry of drugs has received major attention in the last years and has become an increasingly important benchmark in drug development, because solid-dosage forms are the most commonly used preparations.

Active pharmaceutical ingredients (API) may exist in various solid forms, which can lead to differences in the intermolecular interactions, affecting the internal energy and enthalpy, and the degree of disorder, affecting the entropy.[1] The development of new formulations or materials based on a particular API requires a detailed knowledge of the solid form because they can contain the API in a different crystalline form[2] or as an amorphous material, which could affect the interaction with the rest of the components.[3] In fact, different solid forms of an API often lead to differences in physicochemical properties, for example, solubility, dissolution rate, stability, and mechanical properties. Hence, the detailed knowledge of the solid forms of an API is a key element in pharmaceutical development.[4,5]

Morphine (MOR) is an opiate alkaloid widely used to treat severe acute and chronic pain, providing reliable analgesia for centuries.[6] Since it was first marketed in 1827, much of the available information on the solid state of MOR and its salts dates from several decades ago and is particularly scarce for the hydrochloride salt (MOR-HCl), the free base (MOR), and their hydrates. From the chemical point of view, MOR is a zwitterion, with a basic amine group ($pKa = 8.21$) and an acidic phenolic hydroxyl group (OH-C6, $pKa = 6.5$).[7] The high melting point of MOR (254°C-256°C), which is higher than its sulfate salt (250°C), reflects the high cohesive energy of the crystal, which results in a low solubility in both water and lipophilic solvents.[8] The aqueous soluble sulfate pentahydrate salt (mostly used in the United States) and the hydrochloride trihydrate salt (MOR-HCl.3H_2O; Fig. 1) are in regular therapeutic use. In addition, MOR has been used in several developments of pharmaceutical interest.[9]

This article contains supplementary material available from the authors by request or via the Internet at http://dx.doi.org/10.1016/j.xphs.2017.05.021.

* *Correspondence to:* M.E. Olivera (Telephone/Fax: +54 351 5353865).
E-mail address: meoliver@fcq.unc.edu.ar (M.E. Olivera).

http://dx.doi.org/10.1016/j.xphs.2017.05.021
0022-3549/

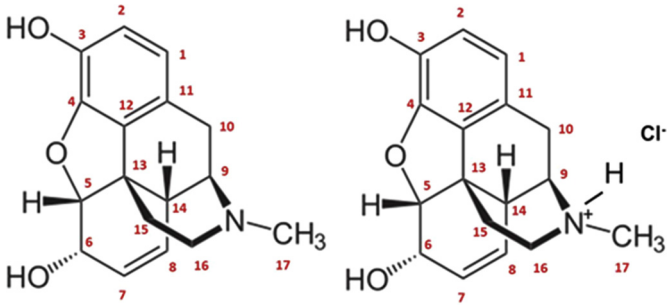

Figure 1. Molecular structure of MOR (left) and MOR-HCl (right).

Although there are recent results on solid state of MOR-related compounds, all these evidence does not allow correlating uniquely with some of its pharmaceutical properties, in particular, the information about the zwitterionic character of MOR crystals is still inconclusive.[8] For example, Baranska and Kaczor[10] have studied MOR using Raman and FTIR spectroscopies. Besides, Guguta et al.[11] have studied MOR, MOR-HCl, and some related hydrated compounds by performing powder X-ray diffraction (PXRD) and solving the structure by numerical programs and obtained information on hydrogen bonds. Information on hydrogen bonds has also been provided by a combination of experimental and computational methods.[12]

Solid-state nuclear magnetic resonance (ssNMR) has become an extremely powerful and versatile technique for the study of drugs in the solid state, particularly useful in pharmaceutical applications, such as characterization of bulk drugs, inclusion complexes, drugs in polymer matrixes, and dosage forms.[13-21] To our knowledge, ssNMR has been applied neither to MOR-HCl.$3H_2O$, which is a commercially available salt in several countries,[22] nor to MOR or MOR-HCl. Considering that the use of MOR is widely extended, the information obtained by ssNMR is particularly relevant because the European Medicines Agency and the Food and Drug Administration have recommended it as one of the reference techniques to determine whether several forms of a drug exist.[23,24] In addition, several new developments based on MOR, resulting in different solid forms, have been proposed in the last years.[25-27] Consequently, ssNMR can provide a wealth of information that cannot be obtained by other means.

The objective of this work was to obtain updated and reliable information about the solid state of MOR-HCl.$3H_2O$ and related anhydrous and free base counterparts using ^{13}C cross-polarization with magic angle spinning (CPMAS) and ^{1}H-^{13}C heteronuclear correlation (HETCOR) ssNMR techniques. FTIR and PXRD spectroscopy, Raman, and thermal analysis were also performed.

Experimental Section

Materials

MOR-HCl.$3H_2O$ was purchased from Droguería Verardo SA, Argentina. MOR.H_2O was obtained by neutralization of MOR-HCl.$3H_2O$ with 2M ammonium hydroxide (Cicarelli, Santa Fe, Argentina). Briefly, 240 mg of MOR-HCl.$3H_2O$ was dissolved with 5 mL of distilled water to obtain a clear solution with a pH of approximately 5. After the addition of an equimolar amount of ammonium hydroxide (0.40 mL), the white solid obtained was separated from the supernatant by filtration and repeatedly rinsed with distilled water until a pH value close to neutral was obtained. Subsequently, the solid was dried to constant weight in an oven at 65°C.

To obtain the anhydrous counterparts, MOR-HCl.$3H_2O$ and MOR.H_2O were dried in an oven at 105°C for 1 h.

Solid-state NMR

High-resolution ^{13}C ssNMR spectra and 2-dimensional (2D) ^{1}H-^{13}C HETCOR spectra for MOR-HCl.$3H_2O$, MOR-HCl, MOR.H_2O, and MOR were recorded at room temperature on a Bruker Avance II NMR spectrometer operating at a resonance frequency of 300.13 MHz for protons and 75.46 MHz for carbons and equipped with a 4-mm magic angle spinning (MAS) probe. One-dimensional (1D) ^{13}C spectra were obtained by performing ramped CPMAS[28,29] technique and using SPINAL-64 heteronuclear decoupling during acquisition.[30] Glycine was used as an external reference for the ^{13}C spectra ($\delta_{COOH} = 176.46$ ppm) and for setting the Harmann−Hahn matching condition in the CP experiments at under 10 kHz of spinning rate. For all the samples, 1024 scans were recorded in order to obtain an adequate signal-to-noise ratio. The cycling time was 5 s and the contact time during CP was 2 ms. SPINAL-64 pulse sequence was used for decoupling during acquisition (82 ms), with a proton field H_{1H} satisfying $\omega_{1H}/2\pi = \gamma_H H_{1H}/2\pi = 60$ kHz.

The nonquaternary suppression spectra (quaternary carbon and methyl group only) were recorded for all the samples at 10 kHz MAS. Following the CP period, a delay of 40 μs was introduced before the acquisition period without applying any radiofrequency pulses on ^{1}H and ^{13}C channels, resulting in a rapid decay for the CH and CH_2 signals due to their strong ^{1}H-^{13}C dipolar couplings. The signals of CH and CH_2 groups can thus be suppressed, leaving only the signals of quaternary carbon and methyl group.[31]

2D ^{1}H-^{13}C HETCOR spectra for all the samples were recorded following the sequence presented by van Rossum et al.[32]The pulse sequence starts with a $(\pi/2+\theta_m)$ pulse on protons, where θ_m is the magic angle, followed by a train of off-resonance frequency-switched Lee-Goldburg (FSLG) pulses[33-35] to cancel the first 2 terms of the ^{1}H-^{1}H dipolar coupling Hamiltonian in the tilted rotating frame. FSLG irradiation was applied during the t_1 evolution time in multiples of the period τ, corresponding to a complete 2π rotation around the tilted axis. After the train of FSLG pulses, the proton magnetization is flipped back in the transverse plane by the magic-angle pulse. A ramped-amplitude CP sequence was used to enhance ^{13}C signals, and the SPINAL-64 pulse sequence was used to decouple protons during ^{13}C signal acquisition. The period τ was set to 7.68 μs. The CP contact time during HETCOR was set to 200 μs to avoid any relayed homonuclear spin-diffusion-type processes, and the recycle delay was 5 s. The duration of the magic-angle pulse was 2.55 μs. The total acquisition time for proton dimension was 1.14 ms corresponding to 64 increments with a dwell time of 35.5 μs. The spinning rate was 10 kHz. The external reference for the chemical shifts in the second dimension (^{1}H) was Adamantane, setting the ^{1}H signal to 1.85 ppm.[36]

Vibrational Spectroscopy

FTIR spectra were recorded in a Vertex 70, Bruker Optics spectrometer equipped with a DTGS detector, a Globar source, and a wide-range beam splitter. A single-reflection diamond attenuated total reflectance (ATR) accessory (Platinum; Bruker Optics) was used. Raman spectra were obtained using a RAM II accessory coupled to the FTIR spectrometer. Samples were excited with an Nd:YAG laser (1064 nm) and the scattered radiation recorded with Ge detector refrigerated with liquid nitrogen. Raman and IR spectra were obtained at a 2 cm^{-1} resolution.

Powder X-Ray Diffraction

Powder X-ray diffractograms were obtained using a D8 Advanced Bruker AXS, equipped with a theta/theta goniometer,

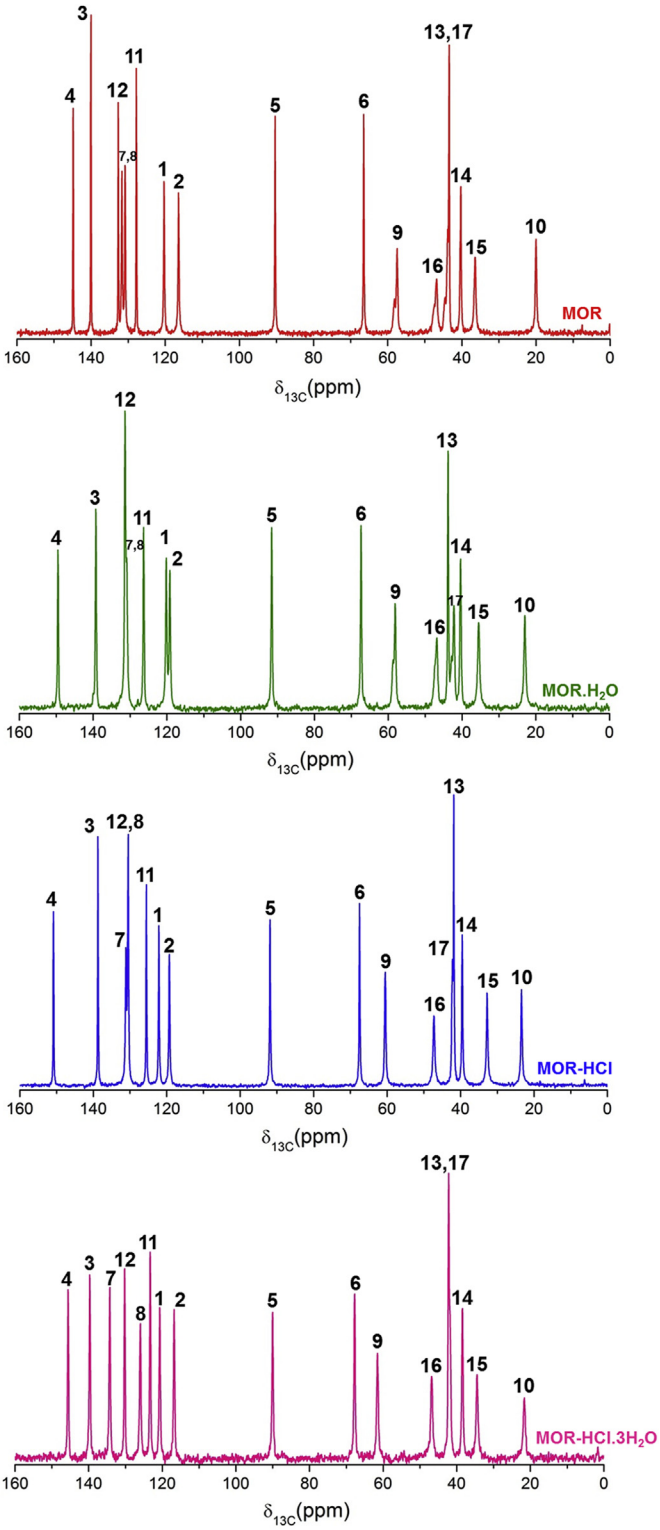

Figure 2. ^{13}C CPMAS spectra for MOR, MOR-HCl, and their hydrates. Carbon numbering corresponds to Figure 1.

operating in the Bragg-Brentano geometry with a fixed specimen holder, Cu Kα (0.15419 nm) radiation source, and a LynxEye detector. The voltage and electric current applied were 40 kV and 40 mA, respectively. The opening of the slit used for the beam incident on the sample was 0.6 mm. The sample was scanned between 5° and 50° using the step scan mode (step 0.02°, integration time 1 s).

Thermal Analysis

Thermogravimetric (TGA) and differential scanning calorimetry (DSC) curves were obtained using a Jupiter STA 449, NETZSCH simultaneous thermal analysis equipment. A sample of around 2 mg was placed in sealed aluminum crucibles with pierced lids. Measurements were made from room temperature up to 350°C using a heating rate of 10°C/min. The sensors and the crucibles were under a constant flow of nitrogen (70 mL/min) during the experiment. The fusion, dehydration, and decomposition temperatures were taken as the extrapolated onset temperature of the endothermic/exothermic peak.

Results and Discussion

^{1}H-^{13}C CPMAS Solid-State NMR

ssNMR provides a direct way to identify and analyze pharmaceutical derivatives to give information of molecular interactions, conformations, or zwitterionic character.[37]

Figure 2 shows the ^{13}C CPMAS spectra for MOR, MOR-HCl, and their hydrates MOR.H_2O and MOR-HCl.3H_2O. Table 1 reports the ^{13}C chemical shifts for all the compounds.

All the compounds have different and well-identified spectra, with well-resolved resonances for the 17 carbons present in MOR. The assignments were performed by comparing reported ^{13}C spectra for MOR in solution[38,39] and reported solid-state ^{13}C spectra for MOR sulfate.[40,41] In addition, the nonquaternary suppression spectra were used to support the assignments of quaternary carbons and methyl groups (Fig. S1, Supporting Information).

A common important feature in all the samples studied in this work is the resonance splitting that can be observed for carbons C9, C16, and C17. These asymmetric doublets are characteristic in high-resolution solid-state spectra of carbons directly bonded to nitrogen (with spins ½ and 1, respectively), that is, the splittings are due to ^{13}C-^{14}N residual dipolar couplings.[42] These resonance splittings have been observed previously for the sulfate salt of MOR.[40,41] The most notable observation in MOR-HCl.3H_2O and MOR-HCl ^{13}C spectra (see Fig. 2 and Table 1) is the reduction of the line splitting in the carbon signals belonging to C9, C16, and C17 which are 35 Hz

Table 1
^{13}C Chemical Shifts (in ppm) Extracted From the ^{13}C CPMAS Spectra in MOR, MOR.H_2O, MOR-HCl, and MOR-HCl.3H_2O

Carbon Number[a]	MOR	MOR.H_2O	MOR-HCl	MOR-HCl.3H_2O
1	120.3	120.2	122.2	120.7
2	116.4	119.2	119.3	116.8
3	140.1	139.3	138.8	139.7
4	144.8	149.5	150.9	145.6
5	90.4	91.6	91.9	90.0
6	66.5	67.4	67.5	67.7
7	131.7	130.9	131.1	134.2
8	130.9	130.9	130.7	126.0
9	57.5, 58.2	58.2, 58.7	60.6	61.5
10	20.0	23.0	23.4	21.7
11	127.8	126.3	125.6	123.3
12	132.7	131.3	130.5	130.2
13	43.5	43.8	41.9	43.2
14	40.3	40.4	39.6	38.5
15	36.4	35.5	32.8	34.5
16	46.8, 47.4	46.8, 47.4	47.3	46.8
17	43.8, 44.4	42.2, 42.8	42.2	41.8

[a] Carbon numbering corresponds to Figure 1.

Table 2
Characteristic Hydrogen Bonds Extracted From Guguta et al.[11] and Braun et al.[12]

Compound	Characteristic HB
MOR-HCl.3H_2O	C6-OH···N
	C3-OH···O (water)
	C6-OH···O (water)
	OH···Cl^-
	OH···O (water)
MOR-HCl	N-H···Cl^-
	C3-OH···Cl^-
	C6-OH···Cl^-
MOR.H_2O	C3-OH···N
	C3-OH···O (water)
	C6-OH···O (water)
MOR	C3-OH···O-C6

smaller in MOR-HCl and its hydrate than in MOR or MOR.H_2O. It is worth to mention that the residual dipolar coupling is proportional to the quadrupolar coupling constant which is related to the electrical field gradient and also depends on the orientation of the principal directions of the electrical field gradient tensor in the molecular frame. Small changes in the C-N distance could also be noticed through changes in the splitting. Then, a change in the electronic distribution of the C-N bond in the case of protonated nitrogen could explain the reduction in the signal splitting for carbons C9, C16, and C17 in MOR-HCl and its trihydrate.

Comparing the carbon resonances between MOR-HCl.3H_2O and MOR-HCl, visible shifts (2-7 ppm) to lower ppm for C2, C4, and C8 and upper ppm for C7 in the hydrated compound can be observed (Table 1). These carbons are in the neighborhood of the hydrogen bonds which are established to Cl^- in the anhydrous case, and with water in the hydrated one (see below in Table 2). In contrast, in MOR and MOR.H_2O, the observed shifts for resonances of C4 and C8 are to lower ppm in the hydrated compound (Table 1). This change in behavior in the shifts arises from the fact that in the hydrated MOR the hydrogen bonds are established with water but in the anhydrous compound the hydrogen bond is intramolecular (see below in Table 2). The ^{13}C spectra of MOR-H_2O show that C2, C4, and C10 show the larger shifts (2-5 ppm) to higher ppm with respect to MOR resonances, giving evidence of a change in the environment on the nearby carbons. Mainly C2 and C4 are close to C3-OH which is involved in intra- or intermolecular hydrogen bonds.[10]

^1H-^{13}C Heteronuclear Correlation

Figure 3 displays the 2D ^1H-^{13}C HETCOR NMR spectra for all the compounds. The ^{13}C spectra observed in the direct dimension corresponds to a short contact time of 200 μs, used during the CP period to allow the developing of short-range HETCOR only. The ^1H projection is shown in the indirect dimension. The 2D spectra reveal well-resolved correlations between carbons and their neighboring protons. This fact enables the assignment of the NMR chemical shifts of the corresponding protons, which are shown in Table 3. Besides, the correlations observed between the quaternary carbons C4, C11, C12 and the nearby protons confirmed the assignments for such carbons.

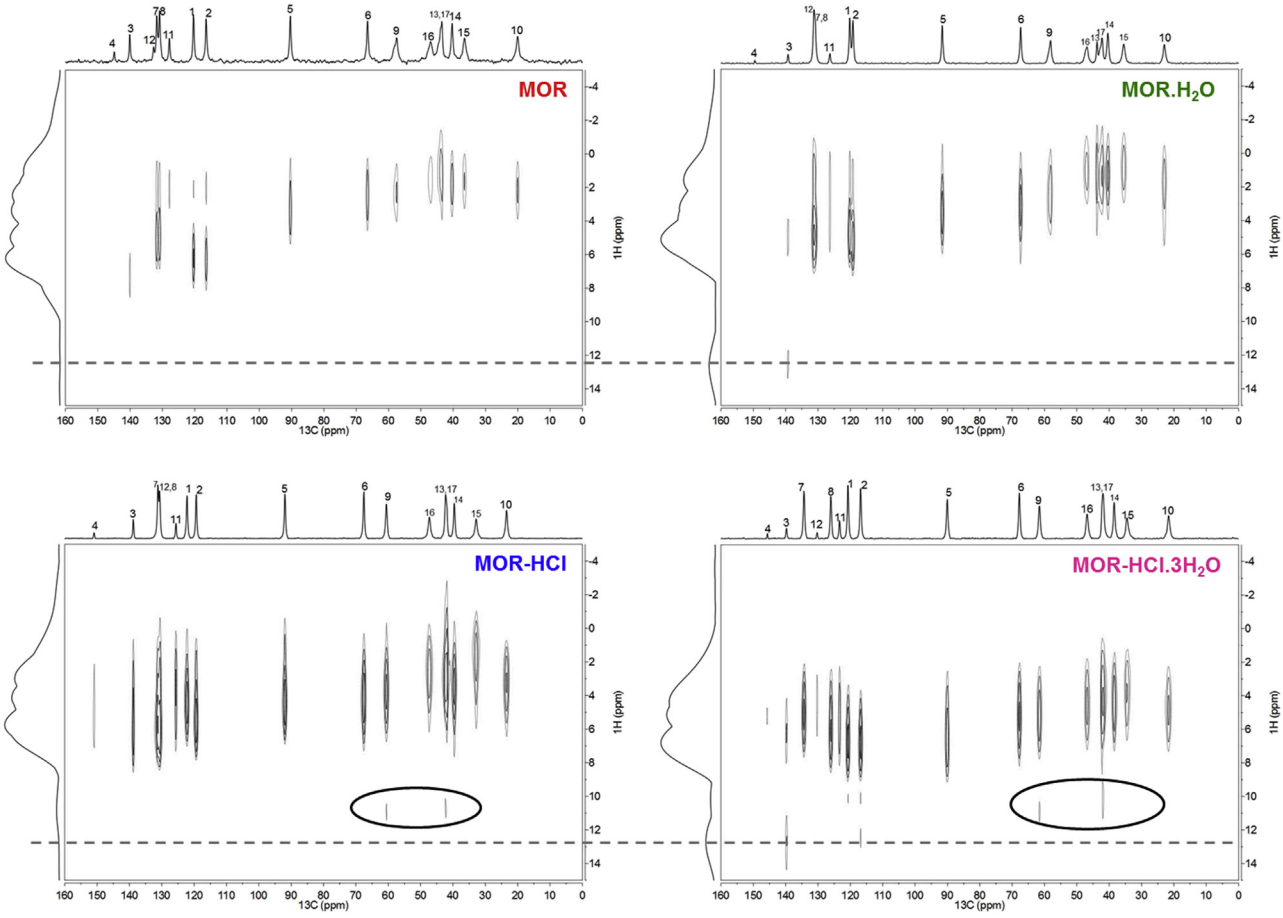

Figure 3. ^1H-^{13}C HETCOR spectra for all the compounds. ^1H spectra are shown in the indirect dimension. ^{13}C spectra correspond to 200 ms of contact time. The circles show the correlation between protons and the carbons bonded to the nitrogen. The dashed lines show the correlation between quaternary C3 and a proton around 12.6 and 12.1 ppm, assigned to the OH proton.

Table 3
^{1}H Chemical Shifts (in ppm) Extracted From the Correlations of the ^{1}H-^{13}C HETCOR Spectra—the Errors Are Around 1 ppm

^{1}H	MOR	MOR.H_2O	MOR-HCl	MOR-HCl.3H_2O
1	6.2	4.9	4.1	6.4
2	6.3	5.5	5.3	5.7
5	3.3	3.8	4.1	6.2
6	2.4	3.3	3.8	4.3
7	5.1	5.2	5.4	5.5
8	4.9	5.2	6.0	5.2
9	2.3	2.7	3.5	4.5
10	2.1	2.0	2.9	4.3
14	1.8	1.6	3.2	3.8
15	1.6	1.1	1.4	3.3
16	1.6	1.2	2.2	4.1
17	1.3	1.6	2.6	3.6
OH-C3	NP	12.6	NP	12.1
NH	NP	NP	10.9	10.1

NP, not present.

The correlations between protons and the carbons bonded to the nitrogen in all the compounds are highlighted in Figure 3. A correlation between C9 and C17 with a proton at about 10.5 ppm, assigned to the NH proton, can be clearly observed in MOR.HCl.3H_2O and MOR-HCl. A less intense correlation with C14 is also present (not shown in Fig. 3 for clarity). Remarkably, these correlations are totally absent in MOR and MOR.H_2O, giving direct evidence that the nitrogen is not protonated in these compounds. As expected, a shift to higher ppm can be seen in the protons close to NH (H9, H14, H15, H16, and H17) in MOR.HCl.3$H_2O$and MOR-HCl (Table 3). These facts confirm that neither MOR nor MOR.H_2O crystallizes as a zwitterion, contrary to that reported by Muhtadi.[8]

Another important correlation is the one between the quaternary carbon C3 and a proton around 12.1 and 12.6 ppm in MOR-HCl.3H_2O and MOR-H_2O, respectively, assigned to the OH-C3 proton. This correlation is absent in MOR-HCl and MOR, suggesting that the hydrogen bonds are placing OH-C3 proton beyond the maximum distance detectable by HETCOR. The presence of water in the molecules reduces the distance between the OH proton and C3, allowing a correlation to be detected by HETCOR experiments. The fact that the OH-C3 proton is involved in hydrogen bonds can be used to distinguish the nature of the hydrogen bonds in hydrate and anhydrate forms.

Previous works in MOR and derivatives, performed by refining results from PXRD data, gave evidence that OH-C3 proton of MOR participates in intramolecular hydrogen bonds, whereas in the hydrate this hydrogen bond occurs with H_2O.[31,32] In Table 2, we have reproduced the results obtained in references.[33,34] In the case of MOR-HCl, hydrogen bonds are mainly with Cl^{-}. Then, the fact that OH is not visible in MOR and MOR-HCl HETCOR spectra gives evidence that the hydrogen bonds in the anhydrate forms have a different nature or strength than in their respective hydrates. Moreover, the changes in the 1D ^{13}C-NMR spectra of MOR compared to MOR.H_2O can be related to the different hydrogen bonds established in both molecules.

Vibrational Spectroscopy

Figure 4 shows the characteristic FTIR spectra of the 4 compounds under study. Table 4 displays the vibrational frequencies (ν) together with their assignments which are in agreement with data previously published.[11,43-45]

In agreement with the protonation observed from ^{1}H-^{13}C HETCOR experiments, a band at 2719 cm^{-1}, assigned to the N-H vibration of the protonated nitrogen of the tertiary amine, can be observed in both MOR-HCl.3H_2O and MOR-HCl spectra (Fig. 4).

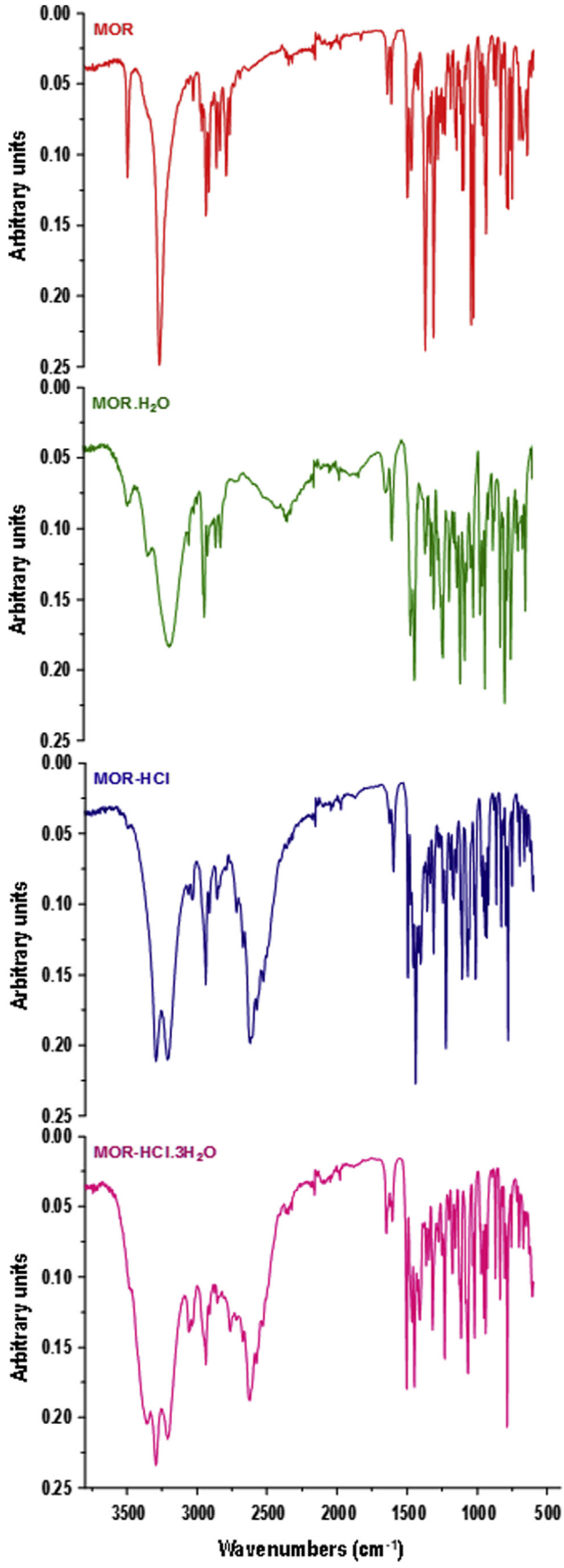

Figure 4. FTIR-ATR spectra of MOR, MOR-HCl, and their hydrates.

Table 4
Assignments and Characteristic Frequencies (cm^{-1}) for MOR, MOR-HCl, MOR.H_2O, and MOR-HCl.$3H_2O$

Assignments	Frequencies (cm^{-1})			
	MOR	MOR.H_2O	MOR-HCl	MOR-HCl.$3H_2O$
O-H (C3 and C6)	3459-3269	3485-3187	3294-3210	3296-3213
C-H stretching	2938, 2917	2939, 2918	2939, 2913	2939, 2912
H_3C-N-H^+ (N-H vibration)	NP	NP	2719	2719
H_3C-N (C-N vibration)	2864-2839	2859-2824	NA	NA
$C_7 = C_8$ and aromatic C=C	1646-1616	1645-1613	1647-1615	1646-1614

NP, not present; NA, not assigned.

In addition, MOR and MOR-HCl show sharp bands around 3500-3200 cm^{-1}, corresponding to the vibration of the OH groups bonded to C3 and C6. As expected, the hydrated counterparts exhibit a new band and also a widening of the previous ones, probably due to the hydrogen bonds favored by the presence of H_2O (Fig. 4).[46]

Furthermore, the bands around 1625 cm^{-1} associated with the stretching of the C=C bonds display distortions (seen in FTIR and Raman) in the hydrated compounds probably due to the close presence of the hydrogen bonds of C6 with the water molecules.

Powder X-Ray Diffraction

The PXRD patterns for MOR-HCl, MOR, and their corresponding hydrates (Fig. 5) were coincident with those calculated from the structures reported in Cambridge Structural Database, previously reported.[47-50] An additional small reflection at 12°θ (which is present in MOR.H_2O) was observed in MOR, suggesting that a small amount of the hydrated phase is present in the sample, probably due to unintentional hydration of MOR during manipulation.

The presence of water produced an increase in crystallinity with respect to the hydrated forms, confirming that water is part of the structure as observed by NMR and FTIR. Water, being a small molecule with great capacity to build hydrogen bonds, can easily form part of the crystal structure, even providing some additional stability.[46]

Thermal Analysis

Figure 6 shows the DSC and TGA results of MOR-HCl, MOR, and their corresponding hydrates.

The DSC curves of MOR-HCl and MOR-HCl.$3H_2O$ show decomposition exotherms together with weight loss in TGA around 300°C, indicating that these compounds do not have a definite melting point. The DSC curve of MOR-HCl.$3H_2O$ exhibits a single broad endotherm at 90.7°C (onset, 74.6°C; enthalpy, 372.7 J/g) associated with a weight loss of 13.6%, which agrees with the expected value for the simultaneous release of the 3 water molecules (14.4%).

All these events are in agreement with DSC and TGA reported for MOR.H_2O and MOR-HCl.$3H_2O$ by Braun et al.,[12] allowing to identify completely the compounds under study.

The DSC of MOR.H_2O shows a wide endotherm at 100.8°C (onset, 95.9°C; enthalpy, 6.44 J/g), paralleled by a weight loss in TGA assigned to the release of 1 molecule of water (experimental, 4%; theoretical, 6%). Dehydration is completed at 118°C. After that event, the TGA and DSC profiles are similar to those of MOR exhibiting melting with decomposition.

The DSC of MOR exhibits 1 acute endotherm at 260.9°C corresponding to its melting point (onset, 259.3; melting enthalpy, 133.3 J/g), followed by an exothermic degradation peak showing weight loss in the corresponding TGA run. In addition, no weight loss was observed in the TGA profile of MOR when heated from room temperature up to fusion, indicating their anhydrous nature. The high melting enthalpy of MOR reflects high cohesion energy in the crystals, approaching to the values informed for some organic zwitterionic compounds.[51] However, our results confirmed that MOR does not crystallize as a zwitterion and, hence, the high

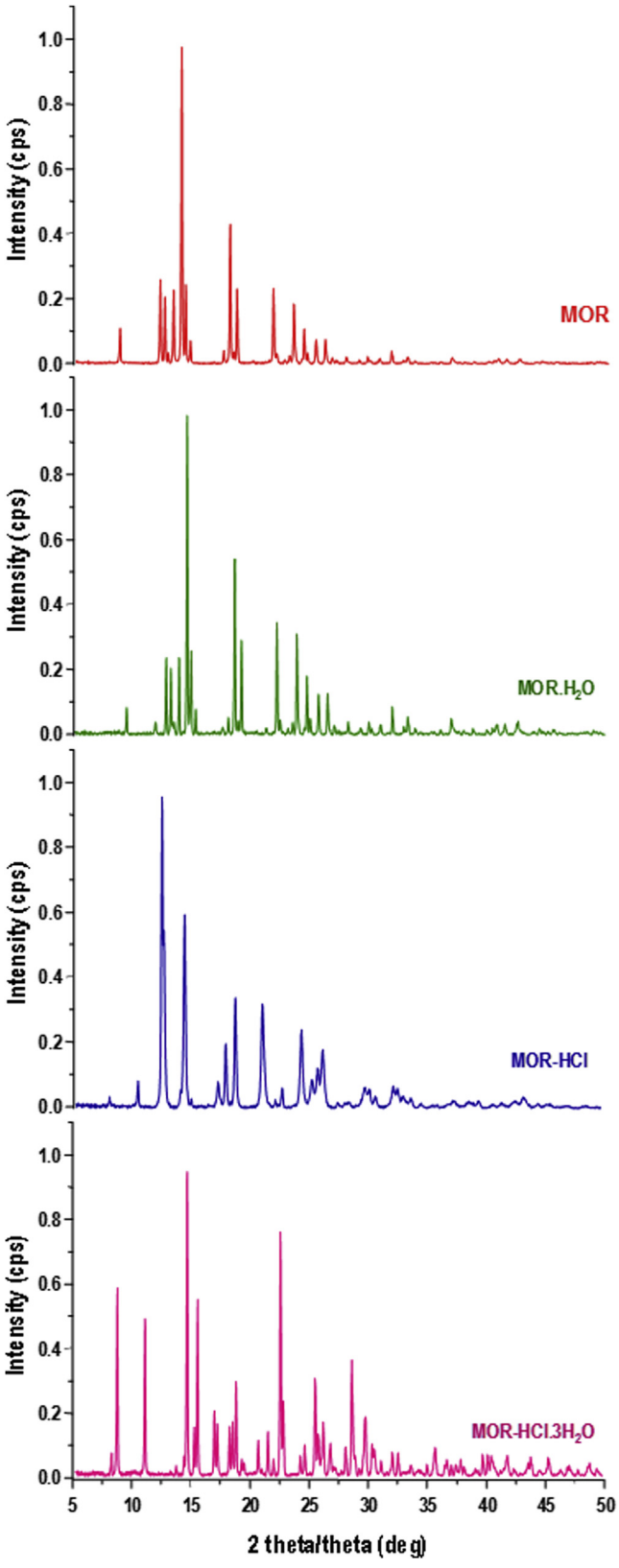

Figure 5. PXRD patterns of MOR, MOR-HCl, MOR.H_2O, and MOR-HCl.$3H_2O$.

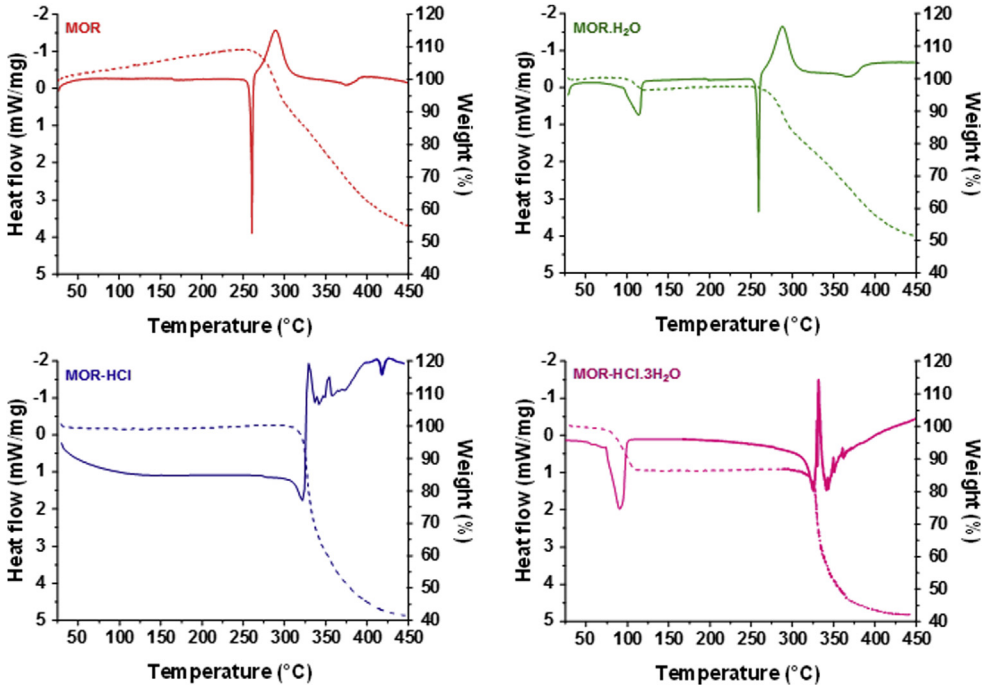

Figure 6. DSC (solid line) and TGA (dashed line) thermograms for MOR, MOR-HCl, and their corresponding hydrates.

cohesion energy can be explained by the number and nature of the hydrogen bonds.

Conclusions

The solid-state characterization of MOR MOR-HCl and their corresponding hydrates was revisited and updated by using IR, DSC, TGA, and X-ray studies. In addition, new information was provided by performing ssNMR advanced techniques. In particular, ^{13}C CPMAS 1D spectra produced a complete identification of the 4 related forms of MOR, distinguishing between all the compounds. Remarkably, the expected splitting in the signals of carbons bonded to ^{14}N quadrupolar nuclei was observed in MOR and its hydrate, whereas in MOR-HCl, this splitting was almost negligible, reflecting different electronic distribution of the C-N bond in MOR and MOR-HCl.

Connecting the information obtained from the 2D ^{1}H-^{13}C HETCOR spectra with FTIR results, we arrived at the confirmation that MOR, in its 2 forms anhydrous or hydrated, is not a zwitterion, in contrast to that proposed in previous reports. The protonation of the nitrogen was evident from the 2D HETCOR experiment, in the hydrochloride and its hydrate, also supported by the IR results. It is not minor to remark that, and although the compound is not zwitterionic, the fact that the OH group was not visible in MOR and MOR-HCl 2D HETCOR gives us strong evidence that the hydrogen bonds in the anhydrate forms have a different nature or strength than in their respective hydrates. These changes in the hydrogen bonds are in agreement with X-ray results previously reported.

The information obtained is relevant for the characterization of MOR as a bulk drug, dosage forms, and future developments.

Acknowledgments

Authors wish to acknowledge the assistance of the Consejo Nacional de Investigaciones Científicas y Técnicas (CONICET-Argentina), Fondo para la Investigación Científica y Tecnológica (FONCyT-Argentina), Universidad Nacional de Córdoba-Argentina, Conselho Nacional de Desenvolvimento Científico e Tecnológico (CNPq-Brazil), Fundação Cearense de Apoio ao Desenvolvimento Científico e Tecnológico (FUNCAP-Brazil), and Coordenação de Aperfeiçoamento de Pessoal de Nível Superior (CAPES-Brazil), which provided support and facilities for this investigation.

References

1. Healy AM, Worku ZA, Kumar D, Madi A. Pharmaceutical solvates, hydrates and amorphous forms: a special emphasis on cocrystals. *Adv Drug Deliv Rev*. 2017 [Epub ahead of print]. http://dx.doi.org/10.1016/j.addr.2017.03.002.
2. Luciani-Giacobbe LC, Ramírez-Rigo MV, Garro-Linck Y, Monti GA, Manzo RH, Olivera ME. Very fast dissolving acid carboxymethylcellulose-rifampicin matrix: development and solid-state characterization. *Eur J Pharm Sci*. 2017;96:398-410.
3. Kini A, Patel SB. Phase behavior, intermolecular interaction, and solid state characterization of amorphous solid dispersion of Febuxostat. *Pharm Dev Technol*. 2017;22(1):45-57.
4. Brittain HG. *Characterization of Pharmaceutical Compounds in the Solid State*. Vol. 10. New York: Academic Press; 2011.
5. Shan-Yang L. Molecular perspectives on solid-state phase transformation and chemical reactivity of drugs: metoclopramide as an example. *Drug Discov Today*. 2015;20(2):209-222.
6. Mazák K, Hosztafi S, Noszál B. Species-specific lipophilicity of morphine antagonists. *Eur J Pharm Sci*. 2015;78:1-7.
7. Lide DR. *CRC Handbook of Chemistry and Physics*. 86th ed. Taylor & Francis Group: CRC Press; 2005.
8. Muhtadi FJ. Morphine. In: Florey K, ed. *Analytical Profiles of Drug Substances*. 1st ed.. London, UK: Academic Press; 1988:259-366; 17.
9. Escudero GE, Romañuk CB, Toledo ME, Olivera ME, Manzo RH, Laino CH. Analgesia enhancement and prevention of tolerance to morphine: beneficial effects of combined therapy with omega-3 fatty acids. *J Pharm Pharmacol*. 2015;67(9):1251-1262.
10. Baranska M, Kaczor A. Morphine studied by vibrational spectroscopy and DFT calculations. *J Raman Spectrosc*. 2012;43:102-107.
11. Guguta C, Peters ThPJ, de Gelder R. Structural investigations of hydrate, anhydrate, free base, and hydrochloride forms of morphine and naloxone. *Cryst Growth Des*. 2008;8(11):4150-4158.
12. Braun DE, Gelbrich T, Kahlenberg V, Griesser UJ. Insights into hydrate formation and stability of morphinanes from a combination of experimental and computational approaches. *Mol Pharmaceutics*. 2014;11:3145-3163.
13. Lutker KM, Quiñones R, Xu J, Ramamoorthy A, Matzger AJ. Polymorphs and hydrates of acyclovir. *J Pharm Sci*. 2011;100(3):949-963.

14. Zhang R, Mroue KH, Ramamoorthy A. Proton chemical shift tensors determined by 3D ultrafast MAS double-quantum NMR spectroscopy. *The J Chem Phy*. 2015;143(14):144201.
15. Nishiyama Y, Zhang R, Ramamoorthy A. Finite-pulse radio frequency driven recoupling with phase cycling for 2D 1H/1H correlation at ultrafast MAS frequencies. *J Magn Reson*. 2014;243:25-32.
16. Chattah AK, Garro-Linck Y, Monti GA, et al. NMR and IR characterization of the aluminium complexes of norfloxacin and ciprofloxacin fluoroquinolones. *Magn Reson Chem*. 2007;45(10):850-859.
17. Romañuk CB, Manzo RH, Garro-Linck Y, Chattah AK, Monti GA, Olivera ME. Characterization of the solubility and solid-state properties of saccharin salts of fluoroquinolones. *J Pharm Sci*. 2009;98(10):3788-3801.
18. Romañuk CB, Garro-Linck Y, Chattah AK, et al. Crystallographic, thermal and spectroscopic characterization of a ciprofloxacin saccharinate polymorph. *Int J Pharm*. 2010;391(1-2):197-202.
19. Garro-Linck Y, Chattah AK, Graf R, et al. Multinuclear solid state NMR investigation of two polymorphic forms of ciprofloxacin-saccharinate. *Phys Chem Chem Phys*. 2011;13(14):6590-6596.
20. Aboul-Enein HY. Applications of solid-state nuclear magnetic resonance spectroscopy to pharmaceutical research. *Spectroscopy*. 1990;5:32-40.
21. Tishmack PA, Bugay DE, Byrn SR. Solid-state nuclear magnetic resonance spectroscopy. Pharmaceutical applications. *J Pharm Sci*. 2003;92(3):441-474.
22. Administración Nacional de Medicamentos, Alimentos y Tecnología Médica. Vademecum Nacional de Medicamentos. Buenos Aires, Argentina: ANMAT, Ministerio de Salud de la Nación. Available at: http://anmatvademecum.servicios.pami.org.ar/index.html. Accessed December 26, 2016.
23. US Government. Food and Drug Administration-FDA. Q6A Specifications: Test Procedures and Acceptance Criteria for New Drug Substances and New Drug Products: Chemical Substances. Federal Register: 2000 (Volume 65, Number 251). Available at: http://www.fda.gov/Drugs/GuidanceComplianceRegulatoryInformation/Guidances/ucm134966.htm. Accessed December 26, 2016.
24. European Medicines Agency-EMA. ICH Topic Q 6 A Specifications: Test Procedures and Acceptance Criteria for New Drug Substances and New Drug Products: Chemical Substances. CPMP/ICH/367/96, 2006. Available at: http://www.ema.europa.eu/docs/en_GB/document_library/Scientific_guideline/2009/09/WC500002823.pdf. Accessed December 26, 2016.
25. Larsen SW, Østergaard J, Poulsen SV, Schulz B, Larsen C. Diflunisal salts of bupivacaine, lidocaine and morphine. Use of the common ion effect for prolonging the release of bupivacaine from mixed salt suspensions in an in vitro dialysis model. *Eur J Pharm Sci*. 2007;31:172-179.
26. Holgado MA, Iruin A, Alvarez-Fuentes J, Fernández-Arévalo M. Development and in vitro evaluation of a controlled release formulation to produce wide dose interval morphine tablets. *Eur J Pharm Biopharm*. 2008;70:544-549.
27. São Pedro A, Fernandes R, Villarreal CF, Fialho R, Cabral Albuquerque E. Opioid-based micro and nanoparticulate formulations: alternative approach on pain management. *J Microencapsulation*. 2016;33(1):1464-5246.
28. Metz G, Wu XL, Smith SO. Ramped-amplitude cross polarization in magic-angle-spinning NMR. *J Magn Reson*. 1994;110:219-227.
29. Harris RK. *Nuclear Magnetic Resonance Spectroscopy: A Physicochemical View*. Essex, UK: Longman Scientific & Technical; 1986.
30. Fung BM, Khitrin AK, Ermolaev K. An improved broadband decoupling sequence for liquid crystals and solids. *J Magn Reson*. 2000;142:97-101.
31. Harris RK. *Nuclear Magnetic Resonance Spectroscopy*. London: Longman Publishing Group; 1986.
32. Van Rossum BJ, Förster H, de Groot HJM. High-field and high-speed CP-MAS ^{13}C NMR heteronuclear dipolar-correlation spectroscopy of solids with frequency-switched Lee–Goldburg homonuclear decoupling. *J Magn Reson*. 1997;124:516-519.
33. Lee M, Goldburg WI. Nuclear magnetic resonance line narrowing by a rotating rf field. *Phys Rev*. 1965;140:A1261-A1271.
34. Bielecki A, Kolbert AC, Levitt MH. Frequency-switched pulse sequences: homonuclear decoupling and dilute spin NMR in solids. *Chem Phys Lett*. 1989;155:341-346.
35. Ramamoorthy A, Wu CH, Opella SJ. Experimental aspects of multidimensional solid-state NMR correlation spectroscopy. *J Mag Res*. 1999;140(1):131-140.
36. Hayashi S, Hayamizu K. Chemical shift standards in high resolution solid state NMR (1) ^{13}C, ^{29}Si, and ^{1}H nuclei. *Bull Chem Soc Jpn*. 1991;64:685-687.
37. Monti GA, Chattah AK, Garro-Linck Y. Solid-state nuclear magnetic resonance in pharmaceutical compounds. *Annu Rep NMR Spectrosc*. 2014;83:221-269.
38. Brown CE, Roerig SC, Fujimoto JM, Burger VT. The structure of morphine differs between the crystalline state and aqueous solution. *J Chem Soc Chem Commun*. 1983;24:1506-1508.
39. Varadi A, Gergely A, Béni S, Jankovics P, Noszál B, Hosztafi S. Sulfate esters of morphine derivatives: synthesis and characterization. *Eur J Pharm Sci*. 2011;42:65-72.
40. Hexem JG, Frey MH, Opella SJ. ^{13}C NMR of crystalline morphine. *J Amer Chem Soc*. 1983;105(18):5717-5719.
41. Kolodziejski W, Klinowski J. Kinetics of cross-polarization in solid-state NMR: a guide for chemists. *Chem Rev*. 2002;102:613-628.
42. Harris RK, Olivieri AC. Quadrupolar effects transferred to spin- 1 2 magic-angle spinning spectra of solids. *Prog Nuc Magn Res Spect*. 1992;4(5):435-456.
43. Rosario-Meléndez RR, Harris CL, Delgado-Rivera R, Yub L, Uhrich KE. Poly-Morphine: an innovative biodegradable polymer drug for extended pain relief. *J Controlled Release*. 2012;162:538-544.
44. Li PW, Zhang J, Zhang L, Mo YJ. Surface-enhanced Raman scattering and adsorption studies of morphine on silver island film. *Vibr Spectr*. 2009;49:2-6.
45. Schulz H, Baranska M, Quilitzsch R, Schütze W. Determination of alkaloids in capsules, milk and ethanolic extracts of poppy (Papaver somniferum L.) by ATR-FT-IR and FT-Raman spectroscopy. *Analyst*. 2004;129:917-920.
46. Shiu Shiang Yang SS, Guillory JK. Polymorphism in sulfonamides. *J Pharm Sci*. 1972;61(1):26-40.
47. Gelbrich T, Braun DE, Griesser UJ. Morphine hydrochloride anhydrate. *Acta Cryst*. 2012;E68:o3358-o3359.
48. Scheins S, Messerschmidt M, Luger L. Submolecular partitioning of morphine hydrate based on its experimental charge density at 25 K. *Acta Cryst*. 2005;B61:443-444.
49. Gelbrich T, Braun DE, Griesser UJ. Stable polymorph of morphine. *Acta Cryst*. 2013;E69:o2.
50. Gylbert L. The crystal and molecular structure of morphine hydrochloride trihydrate. *Acta Cryst*. 1973;B29:1630-1635.
51. Olivera ME, Ramírez Rigo MV, Chattah AK, Levstein PR, Baschini M, Manzo RH. Solution and solid state properties of a set of procaine and procainamide derivatives. *Eur J Pharm Sci*. 2003;18:337-348.